

Magnetic Cross-over in Hexa-coordinate Iron(II) Complexes of Several Schiff Bases

Yonezo MAEDA, Shunji SHITE, Yoshimasa TAKASHIMA, and Yuzo NISHIDA

Department of Chemistry, Faculty of Science 33, Kyushu University, Hakozaki, Higashiku, Fukuoka 812

(Received October 26, 1976)

Iron(II) complexes with the Schiff bases of 6-methyl-2-pyridinecarbaldehyde and 2-quinolinecarbaldehyde, and with α, α' -diimine were prepared. The Mössbauer spectra and magnetic susceptibilities of the complexes, $\text{Fe}(\text{cbi})_2(\text{NCS})_2 \cdot \frac{2}{3}\text{CHCl}_3$, $\text{Fe}(\text{tbi})_2(\text{NCS})_2 \cdot \text{CHCl}_3$, $\text{Fe}(\text{mpmea})_2(\text{ClO}_4)_2$, and $\text{Fe}(\text{mepma})_3(\text{ClO}_4)_2$, were studied in the range of 80—298 K. It was found that these complexes show a $^5\text{T}_2\text{--}^1\text{A}_1$ spin transition in the solid state.

A number of iron(II) complexes have been shown to exhibit a $^5\text{T}_2\text{--}^1\text{A}_1$ spin equilibrium.¹⁻³⁾ In this paper we wish to describe new iron complexes exhibiting such a spin equilibrium. The ligand abbreviations used in this work are as follows.

Abbreviation	Ligand
pbi	<i>N,N'</i> -diphenyl-2,3-butanediimine
tbi	<i>N,N'</i> -di- <i>p</i> -tolyl-2,3-butanediimine
cbi	<i>N,N'</i> -bis(<i>p</i> -chlorophenyl)-2,3-butanediimine
mbi	<i>N,N'</i> -bis(<i>p</i> -methoxyphenyl)-2,3-butanediimine
mepma	<i>N</i> -(6-methyl-2-pyridylmethylene)-methylamine
pmea	<i>N</i> -(2-pyridylmethylene)-2-(2-pyridyl)ethylamine
pema	<i>N</i> -[1-(2-pyridyl)ethylidene]-(2-pyridyl)methylamine
peca	<i>N</i> -[1-(2-pyridyl)ethylidene]-2-(2-pyridyl)ethylamine
mpmma	<i>N</i> -(6-methyl-2-pyridylmethylene)-2-pyridylmethylamine
mpmea	<i>N</i> -(6-methyl-2-pyridylmethylene)-2-(2-pyridyl)ethylamine
qmma	<i>N</i> -(2-quinolylmethylene)-2-pyridylmethylamine
qmea	<i>N</i> -(2-quinolylmethylene)-2-(2-pyridyl)ethylamine

Experimental

The preparation of the 2-quinolinecarbaldehyde was accomplished by the reduction of ω, ω -dibromoquinaldine with silver nitrate.⁴⁾ 6-methyl-2-pyridinecarbaldehyde, 2-pyridyl-

methylamine, and 2-(2-pyridyl)ethylamine were purchased from the Aldrich Co., Ltd. The ligands, α, α' -diimines, were isolated before the preparation of the complexes. The other Schiff bases were used without isolating them as solids. The complexes were prepared by mixing iron(II) salts and the Schiff bases in oxygen-free ethanol. The crude products were recrystallized from chloroform or ethanol. All the complexes except $\text{Fe}(\text{qmma})_2(\text{ClO}_4)_2$ and $\text{Fe}(\text{qmea})_2(\text{ClO}_4)_2$ were generally stable for oxidation.

The analytical data of the complexes prepared are listed in Table 1. The microanalyses were carried out at the Elemental Analysis Center of Kyushu University. The Mössbauer, electronic reflectance, and infrared spectra, and the conductivities in organic solvents were obtained as has been described elsewhere.³⁾ The effective magnetic moments, μ_{eff} , were obtained from the $\mu_{\text{eff}} = 2.83 \sqrt{\chi_m T}$ relation, where χ_m is the molar susceptibility after applying diamagnetic corrections for both the ligands and anions.

Results and Discussion

Characterization of the Samples. The molar conductivities of the complexes listed in Table 2 indicate that the thiocyanates are non-electrolytic in acetone or chloroform, while the perchlorates behave as univalent electrolytes. The infrared spectra of the perchlorates show absorptions around 1090 cm^{-1} , which indicate that the perchlorate ion is ionic in these complexes.

Magnetic Susceptibilities. Figure 1 shows the variation in μ_{eff} with the temperature for the complexes which have cross-over points. Although we observed the Mössbauer absorptions of only low-spin states in

TABLE 1. ANALYTICAL DATA (%)

Complexes	Found				Calcd			
	C	H	N	Fe	C	H	N	Fe
$\text{Fe}(\text{pbi})_2(\text{NCS})_2 \cdot \frac{1}{2}\text{CHCl}_3$	59.27	4.74	12.62	8.05	58.81	4.62	11.93	7.94
$\text{Fe}(\text{tbi})_2(\text{NCS})_2 \cdot \text{CHCl}_3$	56.38	4.97	10.24	6.80	56.97	5.23	10.23	6.81
$\text{Fe}(\text{cbi})_2(\text{NCS})_2 \cdot \frac{2}{3}\text{CHCl}_3$	47.52	3.38	9.62	7.54	48.28	3.33	9.75	7.13
$\text{Fe}(\text{mbi})_2(\text{NCS})_2$	58.58	5.27	10.80	7.55	58.64	5.24	10.99	7.31
$\text{Fe}(\text{pema})_2(\text{ClO}_4)_2$	45.28	3.91	12.07	a)	46.09	3.84	12.41	8.25
$\text{Fe}(\text{peca})_2(\text{ClO}_4)_2$	47.32	4.71	10.91	a)	47.67	4.26	11.91	7.92
$\text{Fe}(\text{pmea})_2(\text{ClO}_4)_2$	45.96	3.91	12.25	a)	46.09	3.84	12.41	8.25
$\text{Fe}(\text{mpmma})_2(\text{ClO}_4)_2 \cdot \text{H}_2\text{O}$	44.29	3.92	11.66	8.46	44.90	4.03	12.09	8.04
$\text{Fe}(\text{mpmea})_2(\text{ClO}_4)_2$	47.20	4.32	11.58	8.26	47.67	4.26	11.91	7.92
$\text{Fe}(\text{qmma})_2(\text{ClO}_4)_2$	51.13	3.79	11.29	6.90	51.96	3.92	11.36	7.46
$\text{Fe}(\text{qmea})_2(\text{ClO}_4)_2$	52.55	3.93	11.72	7.14	53.19	3.91	10.95	7.19
$\text{Fe}(\text{mepma})_3(\text{ClO}_4)_2$	43.62	4.65	12.64	9.15	43.86	4.57	12.79	8.50

a) Was not analyzed.

TABLE 2. MAGNETIC MOMENTS, MOLAR CONDUCTIVITIES, INFRARED SPECTRA, AND REFLECTANCE SPECTRA OF THE IRON COMPLEXES

Compounds	μ_{eff} (BM) at 295 K	Λ_m^a	ν_{NCS} (cm^{-1})	Reflectance data (cm^{-1})
$\text{Fe}(\text{pbi})_2(\text{NCS})_2 \cdot \frac{1}{2}\text{CHCl}_3$	2.87	0 (A)	2070, 2080 2120	29000 s, 15700 s, br, 10500 s
$\text{Fe}(\text{tbi})_2(\text{NCS})_2 \cdot \text{CHCl}_3$	4.26	12.2 (A)	2055 2110	29000 s, 16000 s, br, 10300 s
$\text{Fe}(\text{cbi})_2(\text{NCS})_2 \cdot \frac{2}{3}\text{CHCl}_3$	4.78	0 (C)	2049, 2055	29000 s, 15200 s, br, 10000 s
$\text{Fe}(\text{mbi})_2(\text{NCS})_2$	3.07	0 (C)	2045, 2065 2095, 2110	29000 s, 15700 s, br, 10500
$\text{Fe}(\text{pema})_2(\text{ClO}_4)_2$	1.09	175.9 (A)		24200 s, 20400 sh, 17500 s, br
$\text{Fe}(\text{peca})_2(\text{ClO}_4)_2$	1.07	187.7 (A)		23600, 17100 s, br
$\text{Fe}(\text{pmea})_2(\text{ClO}_4)_2$	1.22	190.0 (A)		25000 s, 19800 sh, 17200 s, br
$\text{Fe}(\text{mpmma})_2(\text{ClO}_4)_2 \cdot \text{H}_2\text{O}$	1.86	163.8 (A)		24400 s, 20400 sh, 17500 s, br, 16800 s, br
$\text{Fe}(\text{mpmea})_2(\text{ClO}_4)_2$	4.38	199.9 (A)		25000 s, 20200 s, 18000 w, sh, 16700 s, br
$\text{Fe}(\text{mepma})_3(\text{ClO}_4)_2$	5.58	213.6 (A)		18500 s, 9400 sh
$\text{Fe}(\text{qmma})_2(\text{ClO}_4)_2$	1.60	b)		b)
$\text{Fe}(\text{qmea})_2(\text{ClO}_4)_2$	5.44	b)		b)

a) $\text{cm}^{-2} \text{ mho mol}^{-1}$ at 25 °C; concn 10^{-3} M in acetone (A) or chloroform (C). b) Was not measured.

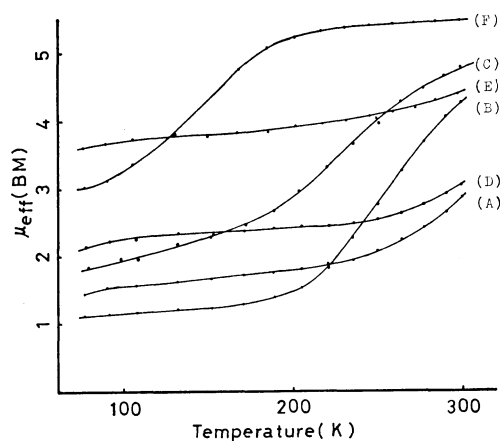


Fig. 1. Variation of the magnetic moment μ_{eff} with temperature for (A) $\text{Fe}(\text{pbi})_2(\text{NCS})_2 \cdot \frac{1}{2}\text{CHCl}_3$, (B) $\text{Fe}(\text{tbi})_2(\text{NCS})_2 \cdot \text{CHCl}_3$, (C) $\text{Fe}(\text{cbi})_2(\text{NCS})_2 \cdot \frac{2}{3}\text{CHCl}_3$, (D) $\text{Fe}(\text{mbi})_2(\text{NCS})_2$, (E) $\text{Fe}(\text{mpmea})_2(\text{ClO}_4)_2$, and (F) $\text{Fe}(\text{mepma})_3(\text{ClO}_4)_2$.

$\text{Fe}(\text{pbi})_2(\text{NCS})_2 \cdot \frac{1}{2}\text{CHCl}_3$ and $\text{Fe}(\text{mbi})_2(\text{NCS})_2$ at 296 K, the magnetic moments of the complexes probably increase at high temperatures, in view of the tendency of the curves. The magnetic data at 295 K show that $\text{Fe}(\text{pmea})_2(\text{ClO}_4)_2$, $\text{Fe}(\text{pema})_2(\text{ClO}_4)_2$, $\text{Fe}(\text{peca})_2(\text{ClO}_4)_2$, $\text{Fe}(\text{mpmma})_2(\text{ClO}_4)_2 \cdot \text{H}_2\text{O}$, and $\text{Fe}(\text{qmma})_2(\text{ClO}_4)_2$ adopt a low-spin configuration (Table 2). A small residual paramagnetism is commonly observed in low-spin iron complexes with imine chelates. A large residual paramagnetism has been observed in the polymorph II of $\text{Fe}(\text{phen})_2(\text{NCS})_2$.⁵⁾ The origin of the rather high paramagnetism of $\text{Fe}(\text{cbi})_2(\text{NCS})_2 \cdot \frac{2}{3}\text{CHCl}_3$, $\text{Fe}(\text{mbi})_2(\text{NCS})_2$, $\text{Fe}(\text{pbi})_2(\text{NCS})_2 \cdot \frac{1}{2}\text{CHCl}_3$, and $\text{Fe}(\text{mpmma})_2(\text{ClO}_4)_2 \cdot \text{H}_2\text{O}$ at low temperatures is not clear.

$\text{Fe}(\text{mpmma})_2(\text{ClO}_4)_2 \cdot \text{H}_2\text{O}$ (five- and five-membered ring) adopts a low-spin configuration, and $\text{Fe}(\text{mpmea})_2$ -

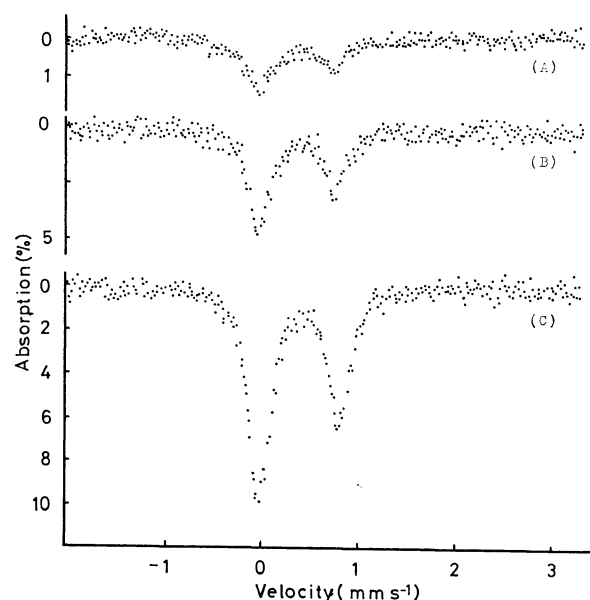


Fig. 2. Mössbauer spectra of $\text{Fe}(\text{pbi})_2(\text{NCS})_2 \cdot \frac{1}{2}\text{CHCl}_3$ at (A) 296 K, (B) 196 K, and (C) 80 K.

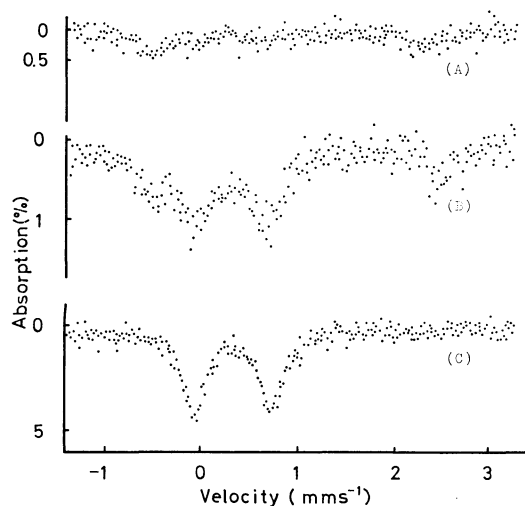
$(\text{ClO}_4)_2$ (five- and six-membered ring) is a cross-over complex. $\text{Fe}(\text{qmma})_2(\text{ClO}_4)_2$ (five- and five-membered ring) and $\text{Fe}(\text{qmea})_2(\text{ClO}_4)_2$ (five- and six-membered ring) adopt low- and high-spin configurations respectively. These facts show that, in the complexes studied here, the ligands fields of the ligands forming five- and five-membered rings are stronger than those of the ligands forming five- and six-membered rings. The change in the spin multiplicity of iron upon the substitution of the methyl group at the 6-position of the pyridine ring is best attributed to the steric effect of methyl.

Mössbauer Spectra. Table 3 shows the Mössbauer parameters of the complexes. The isomer shifts, δ_{Fe} , were measured relative to the center of the spectrum

TABLE 3. MÖSSBAUER PARAMETERS FOR SEVERAL IRON COMPLEXES (mm/s)

Complexes	At 296 K		At 196 K		At 80 K		Spin state
	δ_{Fe}	ΔE	δ_{Fe}	ΔE	δ_{Fe}	ΔE	
Fe(pbi) ₂ (NCS) ₂ · $\frac{1}{2}$ CHCl ₃	a)				a)		<i>S</i> =2
	0.30	0.75			0.38	0.80	<i>S</i> =0
Fe(tbi) ₂ (NCS) ₂ ·CHCl ₃	0.96	2.91	0.99	3.07	a)		<i>S</i> =2
	a)		0.32	0.74	0.37	0.78	<i>S</i> =0
Fe(cbi) ₂ (NCS) ₂ · $\frac{2}{3}$ CHCl ₃	0.87	2.74	1.03	2.92	a)		<i>S</i> =2
	a)		0.34	0.75	0.37	0.78	<i>S</i> =0
Fe(mbi) ₂ (NCS) ₂	a)				a)		<i>S</i> =2
	0.30	0.74			0.38	0.78	<i>S</i> =0
Fe(pema) ₂ (ClO ₄) ₂	0.21	0.98			0.26	0.99	<i>S</i> =0
Fe(peca) ₂ (ClO ₄) ₂	0.25	0.61			0.39	0.80	<i>S</i> =0
Fe(mpma) ₂ (ClO ₄) ₂ ·H ₂ O	0.27	0.94			0.34	1.15	<i>S</i> =0
Fe(mpmea) ₂ (ClO ₄) ₂	0.94	1.92	0.98	2.14	1.02	2.57	<i>S</i> =2
	a)		0.35	0.98	0.35	1.03	<i>S</i> =0
Fe(pmea) ₂ (ClO ₄) ₂	0.32	0.89			0.39	0.89	<i>S</i> =0
Fe(mepma) ₃ (ClO ₄) ₂	1.00	1.06	0.98	1.43	1.09	2.09	<i>S</i> =2
	a)		0.46	0.71	0.48	0.73	<i>S</i> =0
Fe(qmma) ₂ (ClO ₄) ₂	0.31	0.60					<i>S</i> =0
Fe(qmea) ₂ (ClO ₄) ₂	0.94	2.59			1.00	2.96	<i>S</i> =2

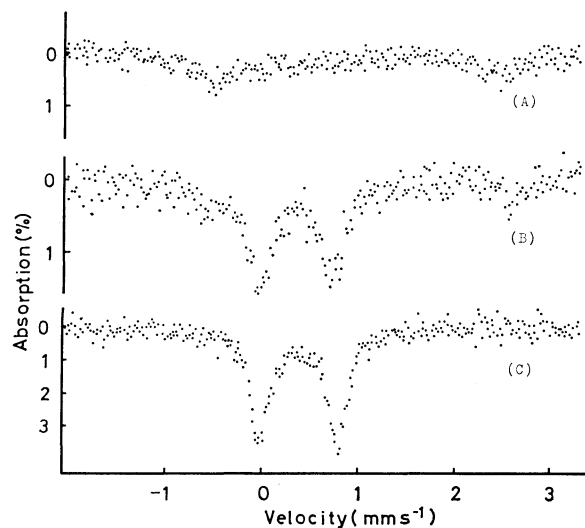
a) Was not observable.

Fig. 3. Mössbauer spectra of Fe(tbi)₂(NCS)₂·CHCl₃ at (A) 296 K, (B) 196 K, and (C) 80 K.

of iron foil. The Mössbauer spectrum of Fe(pbi)₂(NCS)₂· $\frac{1}{2}$ CHCl₃ shows an asymmetric doublet, the center of which is situated in the range of low-spin iron(II) complexes at 296 and 80 K. The Mössbauer spectrum of Fe(mbi)₂(NCS)₂ at 296 K is virtually identical with that of Fe(pbi)₂(NCS)₂· $\frac{1}{2}$ CHCl₃, both giving only a low-spin state, though the former spectrum is not shown here. No spectrum of a high-spin state has been observed because of the small recoilless fraction or small populations of the high-spin isomer at 296 K, as can be seen in Fig. 2.

Fe(tbi)₂(NCS)₂·CHCl₃ and Fe(cbi)₂(NCS)₂· $\frac{2}{3}$ CHCl₃ clearly show the Mössbauer absorptions of the ¹A₁ and ⁵T₂ states at 196 K, as is shown in Figs. 3 and 4.

The Mössbauer spectra of Fe(mpmea)₂(ClO₄)₂ and Fe(mepma)₃(ClO₄)₂ in Figs. 5 and 6 show absorptions

Fig. 4. Mössbauer spectra of Fe(cbi)₂(NCS)₂· $\frac{2}{3}$ CHCl₃ at (A) 296 K, (B) 196 K, and (C) 80 K.

consisting of two species at 80 K, *i.e.*, high-spin and low-spin states. The component of the low-spin configuration increases as the temperature descends.

Assuming that the Debye-Waller factors, $f(^5T_2)$ and $f(^1A_1)$, are equal, we are able to calculate the proportions of the high-spin isomer, $S(^5T_2)$, from the Mössbauer spectral area and the magnetic data respectively. The magnetic moment values for *S*=2 and *S*=0 states were taken to be 5.30 and 0.80 BM for Fe(mpmea)₂(ClO₄)₂, and 5.46 and 0.80 BM for Fe(mepma)₃(ClO₄)₂, respectively. The results are shown below:

Fe(mpmea) ₂ (ClO ₄) ₂ ;	Temp(K)	196	80	14
(from Mössbauer data)	<i>S</i> (⁵ T ₂)(%)	50	45	50
(from magnetic data)	<i>S</i> (⁵ T ₂)(%)	53	45	—

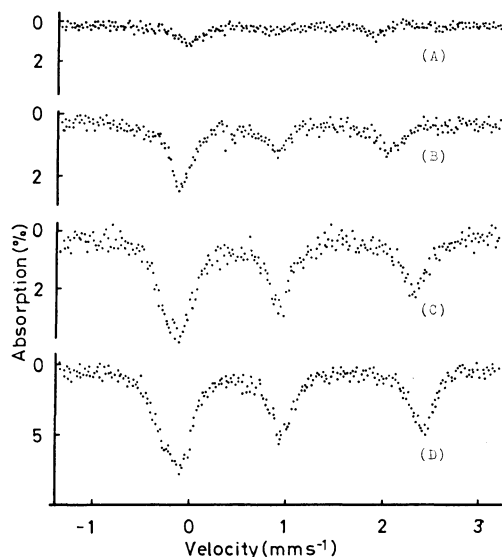


Fig. 5. Mössbauer spectra of $\text{Fe}(\text{mpmea})_2(\text{ClO}_4)_2$ at (A) 296 K, (B) 196 K, (C) 80 K, and (D) 14 K.

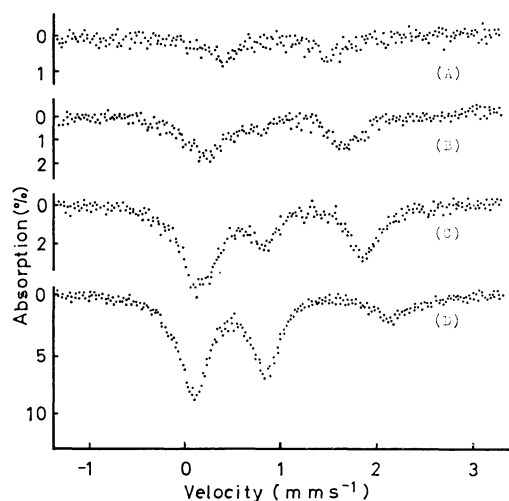


Fig. 6. Mössbauer spectra of $\text{Fe}(\text{mepma})_3(\text{ClO}_4)_2$ at (A) 296 K, (B) 196 K, (C) 147 K, and (D) 80 K.

$\text{Fe}(\text{mepma})_3(\text{ClO}_4)_2$:	Temp(K)	196	147	80
(from Mössbauer data)	$S(^5T_2)(\%)$	68	63	33
(from magnetic data)	$S(^5T_2)(\%)$	91	59	30

The difference between the populations of the high-spin isomer calculated from the Mössbauer spectral area and from the magnetic moment may show that the Debye-Waller factor $f(^5T_2)$ is less than $f(^1A_1)$.

For an axial field resulting from a trigonal ligand symmetry, the quadrupole splitting results primarily from an electron either in $t_{2g}^0(d_z^2)$ or in t_{2g}^\pm , where the t_{2g}^\pm are:

$$t_{2g}^+ = \frac{1}{3}(\sqrt{2}|d_{x^2-y^2}\rangle - |d_{zx}\rangle),$$

$$t_{2g}^- = \frac{1}{3}(\sqrt{2}|d_{xy}\rangle + |d_{yz}\rangle).$$

For the determination of the orbital ground state it is necessary to know the sign of the electric-field gradient tensor (V_{zz}). In $\text{Fe}(\text{mephen})_3(\text{ClO}_4)_2$ ⁶ and $\text{Fe}(\text{2-Cl-phen})_3(\text{ClO}_4)_2$,⁷ negative quadrupole splittings have

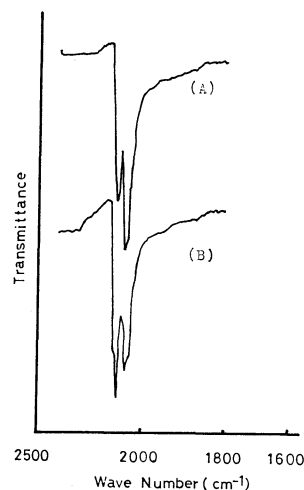


Fig. 7. The C=N stretching vibration region of the infrared spectra of $\text{Fe}(\text{pbi})_2(\text{NCS})_2 \cdot \frac{1}{2}\text{CHCl}_3$ at (A) 340 K and (B) 298 K.

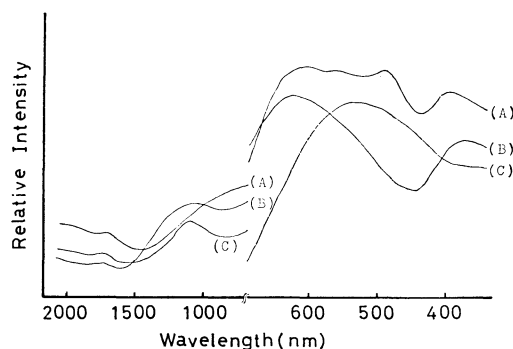


Fig. 8. Electronic reflectance spectra⁷ for (A) $\text{Fe}(\text{mpmea})_2(\text{ClO}_4)_2$, (B) $\text{Fe}(\text{cbi})_2(\text{NCS})_2 \cdot \frac{2}{3}\text{CHCl}_3$, and (C) $\text{Fe}(\text{mepma})_3(\text{ClO}_4)_2$.

been observed. The lowest orbital of $\text{Fe}(\text{mepma})_3(\text{ClO}_4)_2$, therefore, may be d_z^2 . In this state, the field splitting of t_{2g} orbitals increases when the temperature is lowered (*i.e.*, from about 165 cm^{-1} at 296 K to 210 cm^{-1} at 80 K) in Ingall's approximation (assuming $\lambda = -80 \text{ cm}^{-1}$).⁸ This result corresponds to an increasing compression of the coordination octahedron over the 5T_2 - 1A_1 transition region as the temperature descends.

Infrared Spectra. The data in Table 2 show that, in the 5T_2 state, the thiocyanate ion is *N*-bonded.⁹ It has been reported that the C-N stretching modes in the 1A_1 state are observed in the range of 2100–2128 cm^{-1} .¹⁰ Figure 7 shows the infrared spectra of $\text{Fe}(\text{pbi})_2(\text{NCS})_2 \cdot \frac{1}{2}\text{CHCl}_3$ in the range of 1800–2400 cm^{-1} at about 298 and 340 K. The spectrum at 340 K may be considered to be predominantly populated in the 5T_2 ground state, and the spectrum at 298 K, in the 1A_1 ground state.

The splitting of the C-N stretching band has been assigned to a *cis*-configuration of the compound.¹⁰ If $\text{Fe}(\text{tbi})_2(\text{NCS})_2 \cdot \text{CHCl}_3$ (having an unsplit C-N stretching band) had a *trans*-configuration, its quadrupole splitting in the low-spin state would be twice as large as that of the other complexes.¹¹ It seems to be ambiguous, therefore, for the splitting of the $\nu_{\text{C-N}}$ band

to be used to distinguish between *cis*- and *trans*-configurations.

Electronic Spectra. Figure 8 shows the electronic reflectance spectra of several complexes. The positions of the absorption maxima are listed in Table 2. The d-d spectra for α,α -diimine complexes show a shoulder band at about 10500 cm^{-1} . If we take $\Delta(^5T_2) = 10D_q = 10500\text{ cm}^{-1}$, $\Delta(^5T_2)$ should be almost equal to the spin-pairing energy $\pi = \frac{5}{2}B + 4C = 18.5B$ (assuming the usual relation, $C = 4B$, between the electron-repulsion parameters). Thus, taking $\Delta(^5T_2) = \pi$, one obtains $B(^5T_2) = 568\text{ cm}^{-1}$. Since B is 1058 cm^{-1} for free Fe^{2+} , the nephelauxetic ratio is $\beta = B(\text{complex})/B(\text{free ion}) = 0.54$. Since the value of D_q for $\text{Fe}(\text{H}_2\text{O})_6^{2+}$ is estimated to be 1040 cm^{-1} ,¹²⁾ and since the critical D_q has been reported to be in the range of $1160\text{--}1340\text{ cm}^{-1}$, or $1250 \pm 80\text{ cm}^{-1}$,¹³⁾ the D_q for iron-diimine complexes is considered to be significantly small. There are two plausible reasons for the small D_q of the iron-diimine complexes. First, the peak of 10500 cm^{-1} is one component of the doublet, while the other, on the high-energy side, is masked by the stronger charge-transfer band because site symmetry for the metal is distorted from O_h . Second, the Racah parameters for the free metal ion may be reduced drastically by ligand coordination because of the concomitant reduc-

tion of interelectronic repulsions.

References

- 1) H. A. Goodwin, *Coord. Chem. Rev.*, **18**, 293 (1976).
- 2) R. L. Martin and A. H. White, *Trans. Met. Chem.*, **4**, 113 (1968).
- 3) Y. Maeda, Y. Takashima, and Y. Nishida, *Bull. Chem. Soc. Jpn.*, **49**, 2427 (1976).
- 4) D. L. Hammick, *J. Chem. Soc.*, **1926**, 1303.
- 5) E. König, *Coord. Chem. Rev.*, **3**, 471 (1968).
- 6) E. König, G. Ritter, H. Spiering, S. Kremer, K. Madeja, and A. Rosenkranz, *J. Chem. Phys.*, **56**, 3139 (1972).
- 7) W. M. Reiff and G. J. Long, *Inorg. Chem.*, **13**, 2150 (1974).
- 8) R. Ingalls, *Phys. Rev.*, **133**, A787 (1964).
- 9) R. H. Toeniskoetter and S. Solomon, *Inorg. Chem.*, **7**, 617 (1968); P. C. H. Mitchell and R. J. P. Williams, *J. Chem. Soc., A*, **1960**, 1912; J. Lewis, R. S. Nyholm, and P. W. Smith, *ibid.*, **A**, **1961**, 4590.
- 10) E. König, K. Madeja, and K. J. Watson, *J. Am. Chem. Soc.*, **90**, 1146 (1968).
- 11) R. R. Berett and B. W. Fitzsimmons, *J. Chem. Soc., A*, **1967**, 525.
- 12) F. A. Cotton and M. D. Meyers, *J. Am. Chem. Soc.*, **82**, 5023 (1960).
- 13) M. A. Robinson, J. D. Curry, and D. H. Busch, *Inorg. Chem.*, **2**, 1178 (1963).